Selective pharmacologic targeting of CTPS1 shows single-agent activity and synergizes with BCL2 inhibition in aggressive mantle cell lymphoma

Romane Durand, Céline Bellanger, Charlotte Kervoëlen, Benoit Tessoulin, Christelle Dousset, Emmanuelle Menoret, Hélène Asnagli, Andrew Parker, Philip Beer, Catherine Pellat-Deceunynck, et al.

haematologica
Journal of the Ferrata Storti Foundation

Selective pharmacologic targeting of CTPS1 shows single-agent activity and synergizes with BCL2 inhibition in aggressive mantle cell lymphoma

by Romane Durand, Céline Bellanger, Charlotte Kervoëlen, Benoit Tessoulin, Christelle Dousset, Emmanuelle Menoret, Hélène Asnagli, Andrew Parker, Philip Beer, Catherine Pellat-Deceunynck, and David Chiron

Received: September 21, 2023.
Accepted: February 13, 2024.

Citation: Romane Durand, Céline Bellanger, Charlotte Kervoëlen, Benoit Tessoulin, Christelle Dousset, Emmanuelle Menoret, Hélène Asnagli, Andrew Parker, Philip Beer, Catherine Pellat-Deceunynck, and David Chiron. Selective pharmacologic targeting of CTPS1 shows single-agent activity and synergizes with BCL2 inhibition in aggressive mantle cell lymphoma.
Haematologica. 2024 Feb 22. doi: 10.3324/haematol.2023.284345 [Epub ahead of print]

Selective pharmacologic targeting of CTPS1 shows single-agent activity and synergizes with BCL2 inhibition in aggressive mantle cell lymphoma

Romane Durand[1], Céline Bellanger[1], Charlotte Kervoëlen[1], Benoit Tessoulin[2], Christelle Dousset[1], Emmanuelle Menoret[1], Hélène Asnagli[3], Andrew Parker[3], Philip Beer[3], Catherine Pellat-Deceunynck[1], David Chiron[1*]

[1] Nantes Université, Inserm, CNRS, Université d'Angers, CRCI[2]NA, Nantes, France
[2] Nantes Université, CHU de Nantes, Inserm, CNRS, Université d'Angers, CRCI[2]NA, Nantes, France
[3] Step Pharma, Saint-Genis-Pouilly, France

* Corresponding author:

Tel: +33 228080266

Address: 8 quai Moncousu, 44007 Nantes, France

E-mail: david.chiron@univ-nantes.fr

Disclosure

HA, AP and PB are employees of Step Pharma. Other authors declare no competing financial interests.

Running title: Targeting CTPS1 and BCL2 in high-risk MCL

Key words: Mantle Cell Lymphoma, STP-B, Venetoclax, High-risk lymphoma, Cell cycle

Contribution

RD designed and performed the experiments, analyzed data and participated in writing the article. CB performed the experiments and bioinformatics analysis and analyzed data. CD, EM, CK performed experiments and analyzed data. CK and RD performed experiments on NSG mice and analyzed data. BT participated in the design of the study. HA, AP, PB and CPD participated in the design of the study, in the data analysis, and in writing the article. DC designed the study, analyzed data, and wrote the article.

Acknowledgments

The authors would like to thank the patients who agreed to be part of the REFRACT-LYMA cohort and Dr N.L Lilli for cohort management. The authors thank the FINDMED CHICHE ! initiative (ANR-15-CRNT-0007) as well as the Carnot consortium CALYM and the SIRIC ILIAD (INCa-DGOS-Inserm-ITMO Cancer_18011) for their support. We are most grateful to the Genomics Core Facility GenoA, member of Biogenouest and France Genomique and to the Bioinformatics Core Facility BiRD, member of Biogenouest and Institut Français de Bioinformatique (IFB) (ANR-11-INBS-0013) for the use of their resources and their technical support. The authors acknowledge the Cytocell-Flow Cytometry and FACS core facility (SFR Bonamy, BioCore, Inserm UMS 016, CNRS UAR 3556, Nantes, France) for its technical expertise and help.

Data-sharing statement

RNA-sequencing datasets are publicly available in the Gene Expression Omnibus. All other datasets analyzed during the current study are available from the corresponding author on reasonable request.

Abstract

Innovative therapeutic strategies have emerged over the past decade to improve outcomes for most lymphoma patients. Nevertheless, the aggressive presentation seen in high-risk mantle cell lymphoma (MCL) patients remains an unmet medical need. The highly proliferative cells that characterize these tumors depend on nucleotide synthesis to ensure high DNA replication and RNA synthesis. To take advantage of this vulnerability, STP-B, a clinically available small molecule selectively targeting CTP synthase 1 (CTPS1) has been recently developed. CTPS1 is a key enzyme of the pyrimidine synthesis pathway mediated through its unique ability to provide enough CTP in highly proliferating cells. Herein, we demonstrated that CTPS1 was expressed in all MCL cells, and that its high expression was associated with unfavorable outcomes for patients treated with chemotherapy. Using aggressive MCL models characterized by blastoid morphology, *TP53* mutation or polyresistance to targeted therapies, we showed that STP-B was highly effective at nanomolar concentrations *in vitro* and *in vivo*, irrespective of these high-risk features. Inhibition of CTPS1 rapidly leads to cell cycle arrest in early S-phase accompanied by inhibition of translation, including of the anti-apoptotic protein MCL1. Consequently, CTPS1 inhibition induced synergistic cell death in combination with the selective BCL2 inhibitor venetoclax, both *in vitro* and *in vivo*. Overall, our study identified CTPS1 as a promising target for MCL patients and provided a mechanism-based combination with the BCL2 inhibitor venetoclax for the design of future chemotherapy-free treatment regimens to overcome resistance.

Introduction

Since the approval of Imatinib in the early 2000s, dozens of targeted therapies have been developed and are now part of the therapeutic arsenal for solid and hematological malignancies[1]. Identified as Achilles' heels of mature B-cell lymphomas, the selective inhibition of CD20 (i.e., rituximab, obinutuzumab), BCL2 (i.e., venetoclax) and BTK (i.e., ibrutinib, acalabrutinib) has recently led to remarkable clinical activity. These molecules have shown great promise in combination with chemotherapy[2,3], and are now being evaluated in combination as first-line chemotherapy-free regimens[4,5], changing the treatment paradigm for indolent i.e., chronic lymphocytic leukemia (CLL), and aggressive i.e., mantle cell lymphoma (MCL), malignancies. These novel strategies are improving patient survival, but around a third of MCL patients have high-risk disease, which remains associated with rapid relapse and poor outcome[2,6,7]. Biological risk factors characterizing this population, such as high proliferation index (Ki-67), blastoid morphology or *TP53* alterations, are now well described[8]. Nevertheless, aside from the promising initial results obtained with CAR-T cells[9], treatment options for these patients remain an unmet medical need.

Aggressive cancer cells rely on metabolic reprogramming to maintain the hyperactive synthesis of DNA, RNA and phospholipid required to sustain high proliferation and survival[10]. The dependence of MCL cells on high rates of DNA synthesis has been successfully exploited by nucleoside analogs such as cytarabine (ara-C)[11,12]. As the treatment of hematological cancers moves away from chemotherapy towards targeted agents, inhibition of nucleotide synthesis remains an attractive strategy, especially by targeting cytidine triphosphate synthases (CTPS). CTPS1 and 2, key enzymes of the pyrimidine synthesis pathway, catalyze the rate-limiting step of CTP *de novo* synthesis[13,14]. Elevated activity of CTPS in cancer was highlighted decades ago, but strategies to target these enzymes have so far resulted in toxicities and limited efficacies *in vivo*[15,16]. A recent surge of interest has come from our better understanding of the differential role of CTPS1 and 2. Indeed, human

studies have revealed that individuals carrying an inherited homozygous hypomorphic mutation in *CTPS1* display a marked defect in the proliferation of activated T and B cells, with no phenotype outside of the hematopoietic system.[17,18] These studies suggested that the selective inhibition of CTPS1, but not CTPS2, could be an innovative targeted strategy in aggressive lymphoid malignancies. *In vitro* functional studies further confirmed a specific role of CTPS1 and 2 and *in vitro* loss-of-function experiments (CRISPR, shRNA) have demonstrated the dependence of B and T lymphomas, as well as certain solid tumors, on CTPS1 for their proliferation, especially when CTPS2 level is low.[19–23]

STP-B is a highly selective small molecule inhibitor of CTPS1, with more than 1,300-fold selectivity over CTPS2[24]. In the present work, we evaluated the efficacy of pharmacological CTPS1 inhibition as single agent therapy, and in combination with targeted therapies *in vitro* (cell lines, primary cells) and *in vivo* (cell line, PDX), in MCL models displaying high-risk features. Our results demonstrate the efficacy of STP-B in these preclinical models, document its mechanisms of action and highlight a mechanism-based rationale for combination with the BCL2 inhibitor venetoclax.

Methods

Cell culture

Cell lines were authenticated by MHC class I sequencing (EFS Nantes, France) and routinely identified using a flow cytometry-based barcode.[25] Samples were collected from peripheral blood (PB) after obtaining informed consent from MCL patients (REFRACT-LYMA cohort; ethical approval GNEGS-2015-09-1317). MCL cells were enriched using anti-human CD19-conjugated magnetic beads (Miltenyi®) and cultured using previously described protocols.[26]

Drug testing

Cell lines were treated with a highly selective inhibitor of CTPS1 provided by Step Pharma[24], STP-B (1-3000 nM), alone or in combination with venetoclax (0.25-3000 nM) or ibrutinib (5-500 nM). Viability assays (CellTiter-Glo and Annexin-V staining) were performed 24 to 72 h after treatment. The synergy score (Bliss) was calculated using 'SynergyFinder' website. BrdU/PI cell cycle analysis was performed as previously described.[26]

Transcriptomic analysis

Whole transcriptome sequencing of MCL cell lines cultured or not with STP-B, for 24 hours at IC_{50} concentration, and of MCL cells from patients involved in the REFRACT-LYMA cohort, was performed using the 3'seq-RNA Profiling (3'SRP) protocol previously described[27]. Publicly available datasets from bulk and single-cell RNA-seq of MCL samples were also collected from the Gene Expression Omnibus database (GSE93291, GSE239497, GSE239353) and analyzed as previously described[28].

In vivo mouse models

Six to eight-week-old NSG mice (n=40, Charles River) were used for the study. The study was conducted within the UTE (Unité Thérapeutique Expérimentale) animal core facility of IRS-UN (C44-278 certification renewed on December 17, 2015). Animal study was approved

by Ethics Committee of Pays de la Loire, France (review CEEA.2010.49) and the French Ministry of Higher Education and Research and supported by the animal welfare structure of the UTE animal core facility of IRS-UN. The first and most important criteria throughout the study was the animals' health: Any mouse risking to drop 20% of body weight or showing any clinical signs indicating that the animal is not in good health (abnormal behavior, breathing difficulties, coat appearance, etc.) was removed from the study. Venetoclax (InVivoChem) was formulated extemporaneously and protected from light in 5% DMSO / 50% polyethylene glycol300 / 5% Tween80 / 40% ddH2O. STP-B (provided by Step Pharma) was formulated extemporaneously and protected from light in 10% Benzyl alcohol and 90% Castor oil. Z138 and Patient Derived Xenograft (PDX) models used in the study are detailed in the supplementary methods.

Additional methods are detailed in the Online Supplementary Methods section.

Results

A high level of CTPS1, but not CTPS2, is predictive of a poor prognosis in MCL.

While the primary expansion zone of lymphomas is located in the lymph nodes (LN), MCL is characterized by early dissemination in virtually all patients, with lymphoma cells circulating in the bone marrow (BM) and peripheral blood (PB).[29] RNA-seq analysis of primary MCL samples showed that *CTPS1* was expressed at significantly higher levels than *CTPS2* in the LN (n = 100) as well as in circulating cells (n=72) (Fig. 1A, B). A similar expression profile was also observed in MCL cell lines at the RNA (n=11) and protein (n=6) levels (Fig. 1C, Supp Figure S1A).

To further assess the consequences of CTPS expression on clinical outcomes, we studied *CTPS1/2* gene expression in datasets from MCL patients previously treated with chemotherapy (R-CHOP, n=122). Patients with high *CTPS1* expression (upper tercile) had significantly poorer overall survival (OS) with median OS of 0.83 year versus 4.68 years for the lower expressors ($p<0.0001$) (Fig.1D). This observation was confirmed in patients treated with an intensive chemotherapy regimen (R-DHAP, Lyma-trial[30], n=98), in which patients with higher *CTPS1* expression had significantly shorter OS (median not reached, $p=0.037$) (Fig.1E). In contrast, *CTPS2* expression was not significantly associated with OS in either of these cohorts (Fig. 1D-E)

Taken together, *CTPS1*, but not *CTPS2*, is expressed in all MCL cells and high levels are associated with unfavorable outcomes, supporting the rationale for its selective targeting in aggressive forms of MCL.

Selective targeting of CTPS1 by STP-B reduces viability of aggressive MCL cells.

Analysis of the DepMap CRISPR dataset[31] suggested that all B-cell lymphoma cell lines were strictly dependent on CTPS1 but not CTPS2 for growth (dependency score mean: -0.93 vs. 0.00; n=70) (Supp Fig. S1B). Consistent with this, targeting CTPS1 with STP-B, a small

molecule inhibitor with high selectivity for CTPS1 over CTPS2[24], resulted in a dramatic loss of viability in all MCL cell lines tested (n=11, median IC_{50} = 220 nM, range 7-3100 nM), with all but one cell line having an IC_{50} of less than 1 µM (Table 1, Fig. 2A). Response to STP-B was not correlated with *CTPS1/2* mRNA level and was independent of high-risk features such as *TP53* mutation and resistance to venetoclax or ibrutinib (Table 1, Supp Fig. S2A-B). This observation was corroborated by data from resistant isogenic cell lines: ibrutinib-resistant JeKo-1, venetoclax-resistant Maver-1 and Z138 $TP53^{KO}$ (CRISPR/Cas9) cell lines (Figure 2B-C, Supp Fig. S2C Supp Table S1).

The activity of STP-B as a single agent was confirmed *in vivo* using the ibrutinib/venetoclax double-resistant Z138 xenograft model. As shown in Figure 2D, tumor volume was significantly reduced in STP-B-treated mice compared with control mice, with inhibition of tumor growth after STP-B treatment reaching 46% by day 17. Of note, the 30 mg/kg dose of STP-B used was well tolerated by the mice (Supp Fig. S3A). The activity of STP-B as a single agent was confirmed in a disseminated MCL model, using ibrutinib-resistant $TP53^{MUT}$ blastoid PDX cells. Over 60% inhibition of circulating MCL cells (huCD45+ cells) was achieved after 3 cycles of treatment (28 days after engraftment) (Figure 2E, left panel), and a significant gain in survival was observed ($p<0.01$), despite the aggressive phenotype of this model (Figure 2E, right panel). In contrast, the number of mouse PBMCs (huCD45- cells) was not significantly altered by treatment (Supp Fig. S3B).

Overall, these results demonstrated that MCL cells are CTPS1-dependent and that its selective inhibition by STP-B impairs growth of aggressive MCL *in vivo*.

CTPS1 is preferentially expressed in cycling MCL cells and its targeting triggers early S-phase arrest.

To further decipher the consequences of selective CTPS1 inhibition at the molecular level, we performed a transcriptomic analysis in 9 MCL cell lines treated or not with STP-B (IC_{50} for 24 hours) (Supp Fig. S4A). After STP-B treatment, 110 genes showed significantly altered expression (29 up and 81 downregulated; adj $p<0.05$) (Supp Fig. S4B). Functional annotation

highlighted the disruption of transcriptional programs associated with translation (translation, cap-dependent translation) and cell cycle (M phase, anaphase, metaphase, cell cycle checkpoints, cell cycle) (Figure 3A). A deeper analysis of cell cycle associated genes highlighted an enrichment of the transcripts expressed in G1_early-S (e.g., *E2F1/2*, *CDK4*, *PIK3IP1* and genes encoding Cyclin D, E and A) and a decrease of late-S_G2/M associated genes (e.g., *MKI67, PLK1, UBEC2, CDC20* and gene encoding Cyclin B), suggesting that CTPS1 inhibition by STP-B led to S-phase arrest (Figure 3B). Regarding transcription factors, YBX1, MYC and E2F family members (E2F3/4) were predicted to be inhibited by STP-B (TRRUST algorithm), in line with cell cycle modulation and recent studies on CTPS1 regulation[20,21,23]. Using LN gene expression data from two cohorts of MCL patients, we showed that expression of *CTPS1*, but not *CTPS2*, was significantly and positively correlated with the proliferation index Ki67 (*MKI67*, *p<0.0001*) levels (Figure 3C). Such a correlation was also confirmed by scRNA-seq in circulating MCL cells, which are mainly characterized by resting cells and minor cycling subpopulations[28]. Indeed, proliferating BM MCL cells, identified using a previously described cell-cycle signature[28], expressed higher levels of *CTPS1* compared to resting cells (p<0.0001), while *CTPS2* showed low levels in both populations (Figure 3D). Overall, these transcriptomic data showed that *CTPS1* is highly expressed in proliferating cells and that its selective targeting alters cell cycle transit resulting in arrest in early S-phase.

Functional cell cycle analysis (BrdU/PI staining) of MCL cell lines (n=5) further demonstrated that a 24-hour exposure to STP-B resulted in a significant accumulation of early-S phase cells (fold increase: 2.0) and a consequent drop in late S and G2/M cells (fold decrease 0.8 and 0.3, respectively) (Figure 4A). This was confirmed in proliferating MCL primary cells (n=11) (Figure 4B). While cell death remained low 24 hours after CTPS1 inhibition, a cytotoxic effect was observed from 48 hours onwards (LD_{50} <120 nM, n=3) (Figure 4C), highlighting that S-phase arrest was followed by massive cell death in highly proliferative cells *in vitro*.

STP-B synergizes with the cytotoxic BCL2 inhibitor venetoclax.

In vitro combination studies were then undertaken with two targeted therapies widely used in MCL i.e., ibrutinib, a selective BTK inhibitor, and venetoclax, a selective BCL2 inhibitor. The combination STP-B/venetoclax, but not STP-B/ibrutinib, led to supra-additive apoptosis (mean synergy score: 11.8 and -3.2, respectively, n=9) (Figure 5A, Supp Fig.5A-B). In contrast to the BCL2-negative UPN1 cells (synergy score: 0.3), BCL2-positive Z138, JeKo-1 and MINO cells, as well as their associated ibrutinib- and venetoclax-resistant derived cell lines, were synergically killed by the STP-B/venetoclax combination (Supp Fig.5B).

Further experiments demonstrated that pretreatment of the venetoclax-resistant Z138 cells with STP-B resulted in an elevated BCL2 priming at the mitochondrial level (increased cytochrome-C release, $p<0.01$) (Figure 5B). To investigate the molecular mechanisms involved in the observed synergy, we first studied the regulation of the anti-apoptotic proteins MCL1 and BCL-XL, two major venetoclax resistance factors located at the mitochondria[32], in Z138 and JeKo-1 cells treated with STP-B for 24 hours. While BCL2 and BCL-XL protein levels remained unchanged, STP-B treatment resulted in a rapid degradation of MCL1 protein in both cell lines, even at low STP-B concentrations (Figure 5C). Quantitative RT-PCR showed that MCL1 mRNA levels did not significantly change after STP-B treatment, suggesting that a defect in the translational machinery is involved in MCL1 depletion (Supp Fig. S6A). Post-transcriptional inhibition of additional proteins translated from so called weak mRNAs[33,34], such as *CCND1*, *CCND2* and *BIRC5* (Supp Fig. S6B-C), as well as the enrichment of transcriptomic functional annotations related to translation (Figure 3A), supported such a mechanism for MCL1 inhibition by STP-B. Decreased phosphorylation of the cap-dependent translation inhibitor 4E-BP1 upon STP-B treatment further suggested that translation was impaired (Supp Fig. S6D). Finally, puromycin incorporation assay confirmed a reduced protein synthesis upon STP-B treatment in both Z138 and JeKo-1 cell lines (Figure 5D). Overall, these results confirmed that CTPS1 inhibition impaired translation, leading to decreased MCL1 protein levels.

Finally, to address CTPS1/BCL2 dual targeting in aggressive MCL cells *in vivo*, we used the venetoclax resistant Z138 xenograft model. While treatment with venetoclax resulted in limited inhibition of tumor growth, STP-B reduced tumor growth to 71% of control at day 17. The combination was more effective, with tumor inhibition reaching 87% compared to control at day 17. Importantly, the synergy was also observed in the latter stages, with tumor mass in mice treated by STP-B alone increasing 2.3-fold between day 17 to day 22, whereas mice treated by the STP-B/venetoclax combination showed stable disease after all three cycles of treatment (1.2-fold increase from day 17 to day 22) (Figure 5E). Both single and combined compounds were well tolerated, with the mean variation in body weight in all groups being less than 10% (not shown).

Discussion

Despite increasing treatment options, around a third of MCL patients are refractory to chemotherapy and respond poorly to targeted therapies[35]. These high-risk patients are now better characterized, but innovative treatment strategies are still limited[8]. Here we show that targeting nucleotide metabolism by selective inhibition of CTPS1, using the small molecule STP-B, effectively reduces viability in preclinical models of highly aggressive MCL *in vitro* and *in vivo*. STP-B has shown efficacy at nanomolar levels *in vitro*, and in mouse models at concentrations achievable in human patients[24], irrespective of high-risk features such as *TP53* gene deletion or mutation, high proliferation index (Ki-67) or blastoid morphology.

In this study, based on transcriptomic analysis and functional validations, we demonstrated that targeting the pyrimidine synthesis pathway in MCL with STP-B resulted in rapid cell cycle arrest. All MCL cases are characterized by a deregulated cell cycle resulting from Cyclin D overexpression, mainly due to a chromosomal translocation t(11;14)(q13;q32)[36], and additional hits in the cell cycle such as *CDKN2A* deletion are associated with resistance to chemotherapy[37]. This unrestrained proliferation suggested that targeting the cell cycle could be a sustainable strategy, particularly in aggressive MCL, which has been confirmed by the clinical efficacy of CDK4/6 inhibitors[38,39]. Nevertheless, as with many targeted therapies, cancer cells have shown multiple ways of escape, notably through RB1 inactivation, which leads to CDK4/6-independent proliferation[40,41]. In contrast, CTPS1, catalyzing a rate-limiting step in CTP synthesis, is essential for lymphoma growth, as recently demonstrated by gene editing[19,21]. Accordingly, *CTPS1* expression was detected in all MCL samples tested (RNA-seq: n=182), suggesting that *CTPS1* loss is infrequent. In addition, *CTPS1* expression was higher in samples with high proliferation (high *MKI67*) and was also described as higher in ibrutinib-refractory patients, who are characterized by a poor prognosis[7,42]. Taken together, CTPS1 appears to be an appealing target to impair the cell cycle of high-risk lymphomas.

In contrast to *CTPS1*, *CTPS2* was expressed at low levels in MCL, did not correlate with *MKI67* and was not associated with a poor prognosis. Despite sharing 74% homology at the protein level, CTPS1 and CTPS2 have differential roles in cell proliferation. Indeed, a recent study suggests that CTPS2 has weaker enzymatic activities and may be involved in maintaining a basal cellular CTP level, and cannot compensate for the role of CTPS1 in high proliferation[19]. This is consistent with human studies showing that CTPS1 homozygous mutations resulted in the inability of activated lymphocytes to highly proliferate, even in the presence of normal CTPS2 levels[17,18]. On the basis of these data, CTPS2 is unlikely to compensate for the loss of CTPS1 enzymatic activity in tumors treated with STP-B. Nevertheless, given the high plasticity of tumor cells under long-term drug pressure, its level should be carefully monitored in future clinical samples if a CTPS1-targeting refractory patient population emerges. A compound from this chemical series entered clinical development for relapsed refractory B and T lymphomas in 2022 (NCT05463263).

Since CTPS1 inhibition preferentially targets proliferating MCL cells, we next tested the efficacy of the combination with venetoclax, a cell-cycle-independent cytotoxic agent. Venetoclax is a BH3-mimetic that selectively targets BCL2 at the mitochondria and induces rapid apoptosis in lymphoma cells such as MCL cells. BCL2 inhibition has shown good clinical activity as a single agent, but tumor cells have the ability to rapidly develop resistance, especially through the upregulation of other anti-apoptotic proteins such as MCL1[43]. Accordingly, simultaneous inhibition of BCL2 and MCL1, using specific BH3-mimetics, enabled highly effective tumor control in MCL patient-derived xenografts[44]. Unfortunately, direct inhibition of MCL1 by selective BH3 mimetics resulted in unexpected cardiac toxicity[45] and alternative strategies to indirectly neutralize MCL1 are being investigated[46,47]. Here, we demonstrated that inhibition of CTPS1, by altering translation, resulted in rapid inhibition of MCL1, but not BCL2, in MCL cells. MCL1 inhibition led to STP-B/venetoclax synergy *in vitro*, as well as effective tumor control in aggressive mouse models of MCL. These results pave the way for the study of such a combination in the near future,

particularly for high-risk MCL cases which currently have very few effective therapeutic options.

De novo pyrimidine synthesis is controlled upstream by mTORC1/S6K1 through CAD phosphorylation[48]. Here we show that selective downstream targeting of CTPS1 results in inhibition of protein synthesis, at least partly via a decrease in mTORC1 activity (inhibition of 4E-BP1 phosphorylation) (Supp Fig. S6D). These results highlight the complexity of feedback regulation occurring in the mTORC1 pathway, which needs further mechanistic studies to potentially uncover new vulnerabilities in lymphomas.

References

1. Zhong L, Li Y, Xiong L, et al. Small molecules in targeted cancer therapy: advances, challenges, and future perspectives. Signal Transduct Target Ther. 2021;6(1):201.
2. Wang ML, Jurczak W, Jerkeman M, et al. Ibrutinib plus bendamustine and rituximab in untreated mantle-cell lymphoma. N Engl J Med. 2022;386(26):2482-2494.
3. Dreyling M, Doorduijn JK, Gine E, et al. Efficacy and safety of ibrutinib combined with standard First-Line treatment or as substitute for autologous stem cell transplantation in younger patients with mantle cell lymphoma: results from the randomized triangle trial by the european MCL network. Blood. 2022;140(Supplement 1):1-3.
4. Le Gouill S, Morschhauser F, Chiron D, et al. Ibrutinib, obinutuzumab, and venetoclax in relapsed and untreated patients with mantle cell lymphoma: a phase 1/2 trial. Blood. 2021;137(7):877-887.
5. Eichhorst B, Niemann CU, Kater AP, et al. First-Line Venetoclax Combinations in Chronic Lymphocytic Leukemia. N Engl J Med. 2023;388(19):1739-1754.
6. Zhao S, Kanagal-Shamanna R, Navsaria L, et al. Efficacy of venetoclax in high risk relapsed mantle cell lymphoma (MCL)-outcomes and mutation profile from venetoclax resistant MCL patients. Am J Hematol. 2020;95(6):623-629.
7. Martin P, Maddocks K, Leonard JP, et al. Postibrutinib outcomes in patients with mantle cell lymphoma. Blood. 2016;127(12):1559-1563.
8. Scheubeck G, Jiang L, Hermine O, et al. Clinical outcome of Mantle Cell Lymphoma patients with high-risk disease (high-risk MIPI-c or high p53 expression). Leukemia. 2023;37(9):1887-1894.
9. Huang Z, Chavda VP, Bezbaruah R, Dhamne H, Yang D-H, Zhao H-B. CAR T-Cell therapy for the management of mantle cell lymphoma. Mol Cancer. 2023;22(1):67.
10. Vander Heiden MG, DeBerardinis RJ. Understanding the intersections between metabolism and cancer biology. Cell. 2017;168(4):657-669.
11. Tisi MC, Moia R, Patti C, et al. Long-term follow-up of rituximab plus bendamustine and cytarabine in older patients with newly diagnosed MCL. Blood Adv. 2023;7(15):3916-3924.
12. Hermine O, Jiang L, Walewski J, et al. High-Dose Cytarabine and Autologous Stem-Cell Transplantation in Mantle Cell Lymphoma: Long-Term Follow-Up of the Randomized Mantle Cell Lymphoma Younger Trial of the European Mantle Cell Lymphoma Network. J Clin Oncol. 2023;41(3):479-484.
13. Lynch EM, Hicks DR, Shepherd M, et al. Human CTP synthase filament structure reveals the active enzyme conformation. Nat Struct Mol Biol. 2017;24(6):507-514.
14. Van Kuilenburg ABP, Meinsma R, Vreken P, Waterham HR, Van Gennip AH. Identification of a cDNA encoding an isoform of human CTP synthetase. Biochim Biophys Acta. 2000;1492(2-3):548-552.
15. Schimmel KJM, Gelderblom H, Guchelaar HJ. Cyclopentenyl Cytosine (CPEC): An Overview of its in vitro and in vivo Activity. Curr Cancer Drug Targets. 2007;7(5):504-509.
16. Williams JC, Kizaki H, Weber G, Morris HP. Increased CTP synthetase activity in cancer cells. Nature. 1978;271(5640):71-73.
17. Martin E, Palmic N, Sanquer S, et al. CTP synthase 1 deficiency in humans reveals its central role in lymphocyte proliferation. Nature. 2014;510(7504):288-292.
18. Martin E, Minet N, Boschat A-C, et al. Impaired lymphocyte function and differentiation in CTPS1-deficient patients result from a hypomorphic homozygous mutation. JCI Insight. 2020;5(5):e133880.
19. Minet N, Boschat A-C, Lane R, et al. Differential roles of CTP synthetases CTPS1 and CTPS2 in cell proliferation. Life Sci Alliance. 2023;6(9):e202302066.
20. Lin Y, Zhang J, Li Y, et al. CTPS1 promotes malignant progression of triple-negative breast cancer with transcriptional activation by YBX1. J Transl Med. 2022;20(1):1-15.
21. Liang J, Ren Y, Du K, et al. MYC-induced cytidine metabolism regulates survival and drug resistance via cGas□STING pathway in mantle cell lymphoma. Br J Haematol. 2023;202(3):550-565.
22. Wu F, Mao Y, Ma T, et al. CTPS1 inhibition suppresses proliferation and migration in colorectal cancer cells. Cell Cycle. 2022;21(24):2563-2574.
23. Sun Z, Zhang Z, Wang Q-Q, Liu J-L. Combined inactivation of CTPS1 and ATR is synthetically lethal to MYC-overexpressing cancer cells. Cancer Res. 2022;82(6):1013-1024.
24. Asnagli H, Minet N, Pfeiffer C, et al. CTP Synthase 1 Is a Novel Therapeutic Target in Lymphoma. Hemasphere. 2023;7(4):e864.
25. Maïga S, Brosseau C, Descamps G, et al. A simple flow cytometry-based barcode for routine authentication of multiple myeloma and mantle cell lymphoma cell lines. Cytometry. 2015;87(4):285-288.
26. Chiron D, Bellanger C, Papin A, et al. Rational targeted therapies to overcome microenvironment-dependent expansion of mantle cell lymphoma. Blood. 2016;128(24):2808-2818.
27. Charpentier E, Cornec M, Dumont S, et al. 3’ RNA sequencing for robust and low-cost gene expression profiling. Protoc Exch. 2021;10:21203.

28. Decombis S, Bellanger C, Le Bris Y, et al. CARD11 gain of function upregulates BCL2A1 and promotes resistance to targeted therapies combination in B-cell lymphoma. Blood. 2023;142(18):1543-1555.
29. Ferrer A, Salaverria I, Bosch F, et al. Leukemic involvement is a common feature in mantle cell lymphoma. Cancer. 2007;109(12):2473-2480.
30. Le Gouill S, Thieblemont C, Oberic L, et al. Rituximab after autologous stem-cell transplantation in mantle-cell lymphoma. N Engl J Med. 2017;377(13):1250-1260.
31. Dempster JM, Rossen J, Kazachkova M, et al. Extracting biological insights from the project achilles genome-scale CRISPR screens in cancer cell lines. BioRxiv. 2019 July 31. doi:10.1101/720243 [preprint, not peer-reviewed]
32. Chiron D, Dousset C, Brosseau C, et al. Biological rational for sequential targeting of Bruton tyrosine kinase and Bcl-2 to overcome CD40-induced ABT-199 resistance in mantle cell lymphoma. Oncotarget. 2015;6(11):8750.
33. Thus YJ, De Rooij MFM, Swier N, et al. Inhibition of casein kinase 2 sensitizes mantle cell lymphoma to venetoclax through MCL-1 downregulation. Haematologica. 2022;108(3):797-810.
34. Descamps G, Gomez-Bougie P, Tamburini J, et al. The cap-translation inhibitor 4EGI-1 induces apoptosis in multiple myeloma through Noxa induction. Br J Cancer. 2012;106(10):1660-1667.
35. Jain P, Wang ML. Mantle cell lymphoma in 2022 - A comprehensive update on molecular pathogenesis, risk stratification, clinical approach, and current and novel treatments. Am J Hematol. 2022;97(5):638-656.
36. Martín-Garcia D, Navarro A, Valdés-Mas R, et al. CCND2 and CCND3 hijack immunoglobulin light-chain enhancers in cyclin D1- mantle cell lymphoma. Blood. 2019;133(9):940-951.
37. Malarikova D, Berkova A, Obr A, et al. Concurrent TP53 and CDKN2A gene aberrations in newly diagnosed mantle cell lymphoma correlate with chemoresistance and call for innovative upfront therapy. Cancers. 2020;12(8):2120.
38. Martin P, Bartlett NL, Blum KA, et al. A phase 1 trial of ibrutinib plus palbociclib in previously treated mantle cell lymphoma. Blood. 2019;133(11):1201-1204.
39. Chiron D, Di Liberto M, Martin P, et al. Cell-cycle reprogramming for PI3K inhibition overrides a relapse-specific C481S BTK mutation revealed by longitudinal functional genomics in mantle cell lymphoma. Cancer Discov. 2014;4(9):1022-1035.
40. Condorelli R, Spring L, O'shaughnessy J, et al. Polyclonal RB1 mutations and acquired resistance to CDK 4/6 inhibitors in patients with metastatic breast cancer. Ann Oncol. 2018;29(3):640-645.
41. Malarikova D, Jorda R, Dolníková A, et al. Cyclin-Dependent Kinase 4/6 Inhibitor Palbociclib Synergizes with BH3-Mimetics in Experimental Models of Relapsed/Refractory Mantle Cell Lymphoma. Blood. 2022;140(Supplement 1):5996-5997.
42. Zhang L, Yao Y, Zhang S, et al. Metabolic reprogramming toward oxidative phosphorylation identifies a therapeutic target for mantle cell lymphoma. Sci Transl Med. 2019;11(491):eaau1167.
43. Thus YJ, Eldering E, Kater AP, Spaargaren M. Tipping the balance: toward rational combination therapies to overcome venetoclax resistance in mantle cell lymphoma. Leukemia. 2022;36(9):2165-2176.
44. Prukova D, Andera L, Nahacka Z, et al. Cotargeting of BCL2 with venetoclax and MCL1 with S63845 is synthetically lethal in vivo in relapsed mantle cell lymphoma. Clin Cancer Res. 2019;25(14):4455-4465.
45. Rasmussen ML, Taneja N, Neininger AC, et al. MCL-1 inhibition by selective BH3 mimetics disrupts mitochondrial dynamics causing loss of viability and functionality of human cardiomyocytes. iScience 2020;23(4):101015.
46. Zhao X, Ren Y, Lawlor M, et al. BCL2 Amplicon Loss and Transcriptional Remodeling Drives ABT-199 Resistance in B Cell Lymphoma Models. Cancer Cell. 2019;35(5):752-766.
47. Zhao X, Bodo J, Chen R, et al. Inhibition of cyclin□dependent kinase 9 synergistically enhances venetoclax activity in mantle cell lymphoma. EJHaem. 2020;1(1):161-169.
48. Ben-Sahra I, Howell JJ, Asara JM, Manning BD. Stimulation of de novo pyrimidine synthesis by growth signaling through mTOR and S6K1. Science. 2013;339(6125):1323-1328.

STP-B	**IC_{50} values (µM)**		RNA-Seq (log2)		Characteristics		Other Drug responses	
MCL cell lines	Mean	SEM	*CTPS1*	*CTPS2*	EBV	*TP53*	Venetoclax	Ibrutinib
Z138	**0.007**	0.00	6,3	2,3	-	wt	R	R
SP53	**0.019**	0.01	6,3	3,5	-	wt	R	S
HBL2	**0.032**	0.01	6,9	2,7	-	D281G	S	R
JeKo-1	**0.036**	0.001	5,5	3,0	-	V122*	R	S
UPN1	**0.082**	0.01	7,8	3,7	-	E286K	R	S
MAVER-1	**0.22**	0.07	6,6	3,5	-	D281E	S	R
REC-1	**0.44**	0.10	6,6	3,1	-	G244D	R	S
GRANTA-519	**0.52**	0.11	7,3	3,2	+	wt	S	R
NTS-3	**0.63**	0.11	5,4	3.8	-	wt	S	S
JVM2	**1.0**	0.47	ND	ND	+	wt	R	S
MINO	**3.1**	0.84	5,9	3,5	-	V147G	S	S

Table 1 _ STP-B IC_{50} and mantle cell lymphoma cell lines characteristics. IC_{50} values were determined by Cell-Titer Glo assay in 11 mantle cell lymphoma (MCL) cell lines treated for 72 hours. Values represent the mean of 3 independent experiments. R: resistant (IC_{50} > 1000 nM), S: sensitive (IC_{50} < 1000 nM). ND: not determined.

Figure Legends

Figure 1: *CTPS1*, but not *CTPS2*, is highly expressed in mantle cell lymphoma and associated with poor prognosis. (A) *CTPS1* and *CTPS2* expression was assessed by RNA-seq in lymph node (LN) biopsies from 100 mantle cell lymphoma (MCL) patients at diagnosis. **(B)** *CTPS1*/2 mRNA levels were analyzed by 3'SRP in MCL cells from bone marrow (BM, n=9) or peripheral blood (PB, n=63) patient samples. **(C)** *CTPS1/2* expression was determined in 11 MCL cell lines (CL) by 3'SRP. Mann-Whitney test was used. ** *p<0.01,* **** *p<0.0001.* **(D)** Overall survival probabilities with different *CTPS1/2* expression were estimated by the Kaplan-Meier method. Probabilities were calculated on 122 MCL patients treated with R-CHOP (public dataset GSE93291). **** *p<0.0001.* **(E)** Overall survival probabilities with different *CTPS1/2* expression were assessed similarly using data from the LYMA trial (n=98). * *p<0.05.*

Figure 2: Selective CTPS1 targeting reduces tumor viability in aggressive mantle cell lymphoma preclinical models.

(A) Dose response to STP-B was evaluated by CellTiter-Glo (CTG) assay in 11 mantle cell lymphoma (MCL) cell lines treated for 72 hours. **(B)** Response to STP-B was similarly assessed in JeKo-1 and a derived ibrutinib-resistant JeKo-1 (left graph) and in MAVER-1 and a derived venetoclax-resistant MAVER-1 (right graph). **(C)** Dose response to STP-B was evaluated by CTG assay in two Z138 $TP53^{KO}$ clones compared to isogenic Z138 $TP53^{WT}$ cells treated for 72 hours. **(D)** STP-B efficacy was determined *in vivo* using Z138 xenograft model. Mice were treated with vehicle (n=5) or 30 mg/kg STP-B (n=5) 4 consecutive days a week for 3 cycles. Tumor size was measured by caliper. **(E)** STP-B efficacy *in vivo* was assessed using a disseminated PDX model (ibrutinib-resistant, $TP53^{MUT}$, blastoid). Left panels: circulating MCL cells count was determined by flow cytometry (huCD45+) 21 days and 28 days after engraftment. Mann-Whitney test was used. ** *p<0.01*. Right panel: survival of PDX mice treated with vehicle (n=5) or STP-B (n=5) was analyzed. Mantel-Cox and Gehan-Breslow-Wilcoxon tests were performed.

Figure 3. CTPS1 is preferentially expressed in cycling mantle cell lymphoma cells and its inhibition affects cell cycle related transcriptional programs.

(A) 9 mantle cell lymphoma (MCL) cell lines were treated with STP-B at IC_{50} for 24 hours and genes expression was determined by 3'SRP. The top 10 enriched Reactome pathways modulated upon STP-B treatment in MCL cells are depicted. **(B)** Cell cycle associated genes expression was analyzed upon STP-B treatment. RNA level fold changes (STP-B/untreated) were calculated for genes involved in G1/early-S phases and late-S/G2/M phases. **(C)** *CTPS1*/*2* expression was compared to *MKI67* expression in LN biopsies from MCL patients using either RNA-seq data (n=98, upper panels) or gene expression profiling data (n=122, lower panels). Spearman test was used. **(D)** *CTPS1* and *CTPS2* levels were assessed by single-cell RNA-seq in highly proliferating and resting cells from 6 bone marrow samples from MCL patients (red line: median).

Figure 4: CTPS1 inhibition results in rapid early S-phase arrest followed by late cell death in mantle cell lymphoma.

(A) Cell cycle analysis (BrdU/PI) was performed in 5 mantle cell lymphoma (MCL) cell lines treated for 24 hours with STP-B at IC_{50}. Percentage of cells in G1, early-S, late-S and G2/M phases is indicated. Change in cell cycle distribution was calculated. Paired t-test was used. * *p<0.05, ** p<0.01, **** p<0.0001.* **(B)** BrdU/PI analysis was performed in 11 MCL primary samples. Primary cells were co-cultured for 72 hours with L40 cells and cytokines to mimic tumor microenvironment and stimulate cell proliferation prior to STP-B treatment (100 nM) for 24 hours. Change in cell cycle distribution was calculated. Paired t-test was used. ** *p<0.01.* **(C)** Cytotoxic activity of STP-B was evaluated at 24, 48 and 72 hours by Annexin-V staining in 3 MCL cell lines. Graphs represent 4 independent experiments.

Figure 5: CTPS1 inhibition synergizes with BCL2 inhibition *in vitro* and *in vivo*.

(A) Bliss synergy scores were determined after treatment for 72 hours with STP-B/venetoclax or STP-B/ibrutinib combinations in mantle cell lymphoma (MCL) cell lines. Detailed results are shown in Supp Fig. S5. **(B)** BCL2 dependence following STP-B treatment was assessed by BH3 profiling in Z138. Cells were pre-treated for 24 hours with 50 or 500 nM STP-B. Cytochrome C release was analyzed after treatment with 10 or 20 µM of venetoclax (BCL2-i) as indicated in Supplemental Methods section. Graph represents 4 independent experiments. Paired t-test was used. * *p<0.05, ** p<0.01*. **(C)** Immunoblotting of anti-apoptotic BCL2 family members was performed in Z138 and JeKo-1 treated with STP-B at 50 and 500 nM for 24 hours. Protein levels normalized to GAPDH level are indicated. **(D)** Puromycin incorporation assay was performed to directly evaluate the rate of protein synthesis upon STP-B treatment. Cells were pre-treated for 24 hours with 50 or 500 nM STP-B, prior to puromycin addition as indicated in Supplemental Methods section. Graph indicates the percentage of puromycin incorporated. **(E)** The efficacy of STP-B/venetoclax combination was evaluated *in vivo* using a Z138 xenograft model (n=5 mice per group). STP-B was dosed at 30 mg/kg days 1-4 of a 7-day cycle and venetoclax was dosed at 75 mg/kg days 2-5 of a 7-day cycle for 3 cycles. Statistical analysis was made using a two-way ANOVA test followed by a Tukey's multiple comparisons test. ** *p<0.01*, **** *p<0.0001*

Figure 1

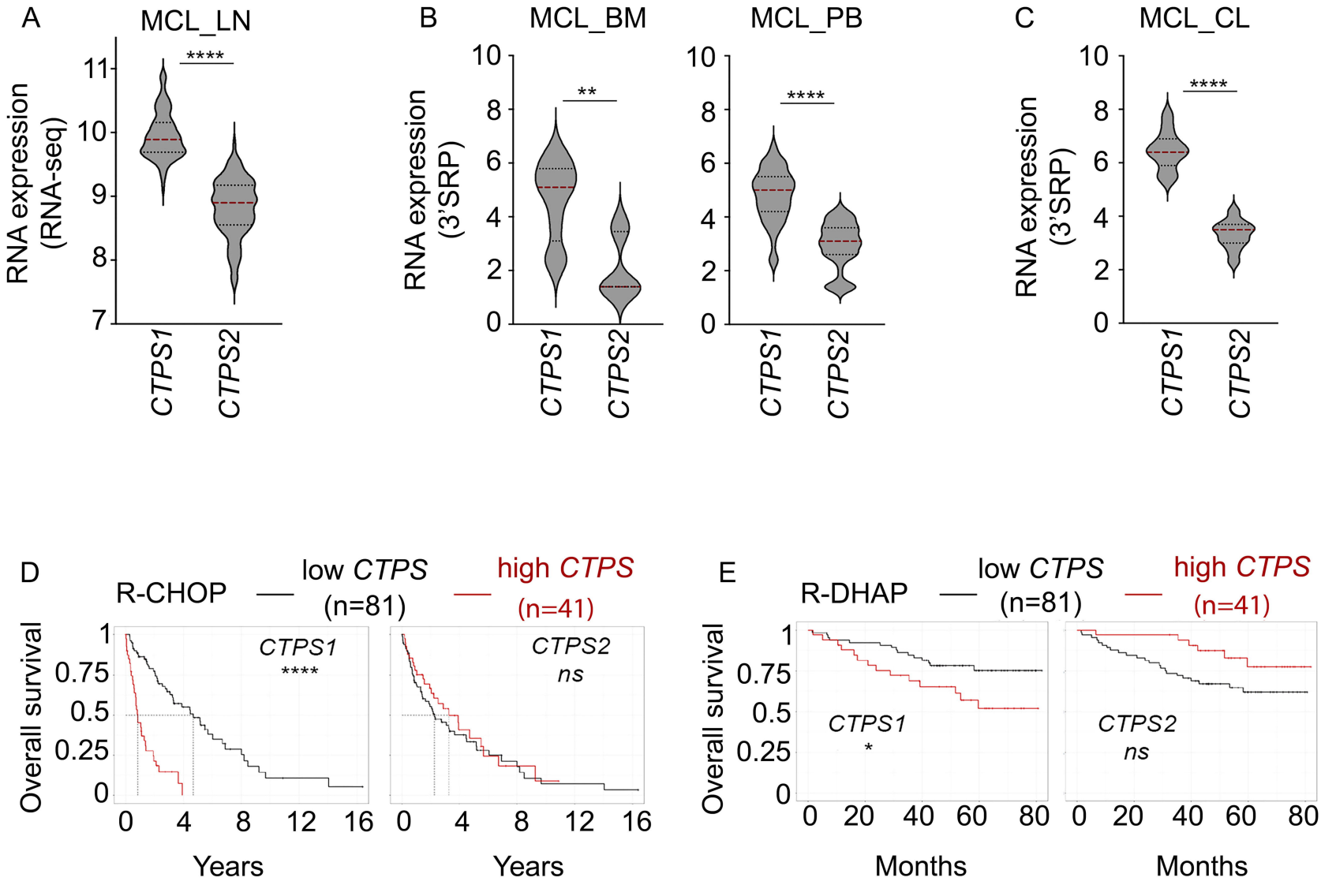
A
MCL_LN
RNA expression (RNA-seq)
****
CTPS1
CTPS2
B
MCL_BM
RNA expression (3'SRP)
**
CTPS1
CTPS2
MCL_PB
****
CTPS1
CTPS2
C
MCL_CL
RNA expression (3'SRP)
****
CTPS1
CTPS2
D
R-CHOP
low CTPS (n=81)
high CTPS (n=41)
Overall survival
CTPS1
****
CTPS2
ns
Years
Years
E
R-DHAP
low CTPS (n=81)
high CTPS (n=41)
Overall survival
CTPS1
*
CTPS2
ns
Months
Months

Figure 2

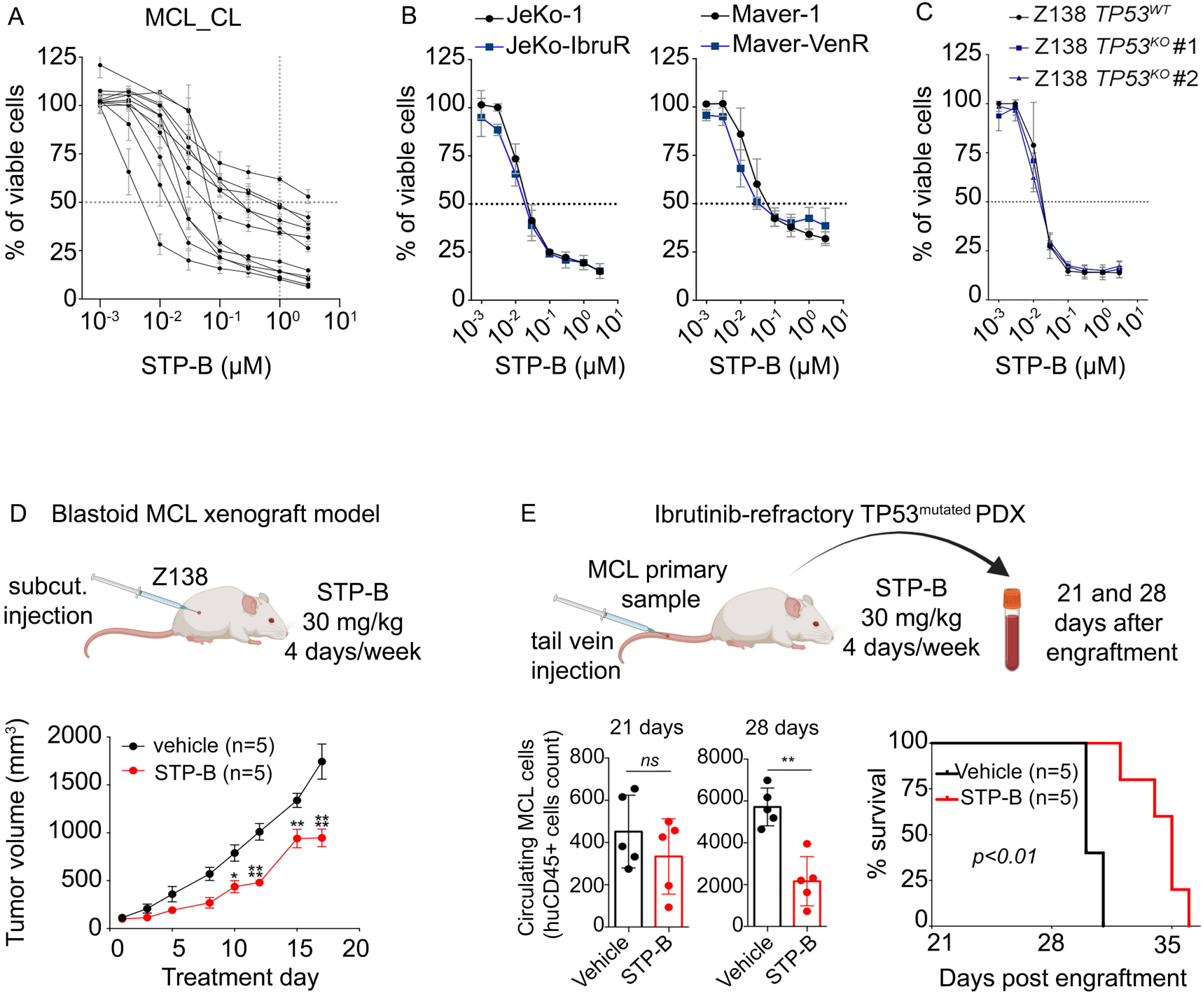
A
MCL_CL
% of viable cells
STP-B (μM)
B
JeKo-1
JeKo-IbruR
Maver-1
Maver-VenR
C
Z138 TP53WT
Z138 TP53KO #1
Z138 TP53KO #2
D
Blastoid MCL xenograft model
subcut. injection
Z138
STP-B 30 mg/kg 4 days/week
Tumor volume (mm3)
vehicle (n=5)
STP-B (n=5)
Treatment day
E
Ibrutinib-refractory TP53mutated PDX
MCL primary sample
tail vein injection
STP-B 30 mg/kg 4 days/week
21 and 28 days after engraftment
Circulating MCL cells (huCD45+ cells count)
21 days
28 days
ns
Vehicle
STP-B
% survival
p<0.01
Days post engraftment

Figure 3

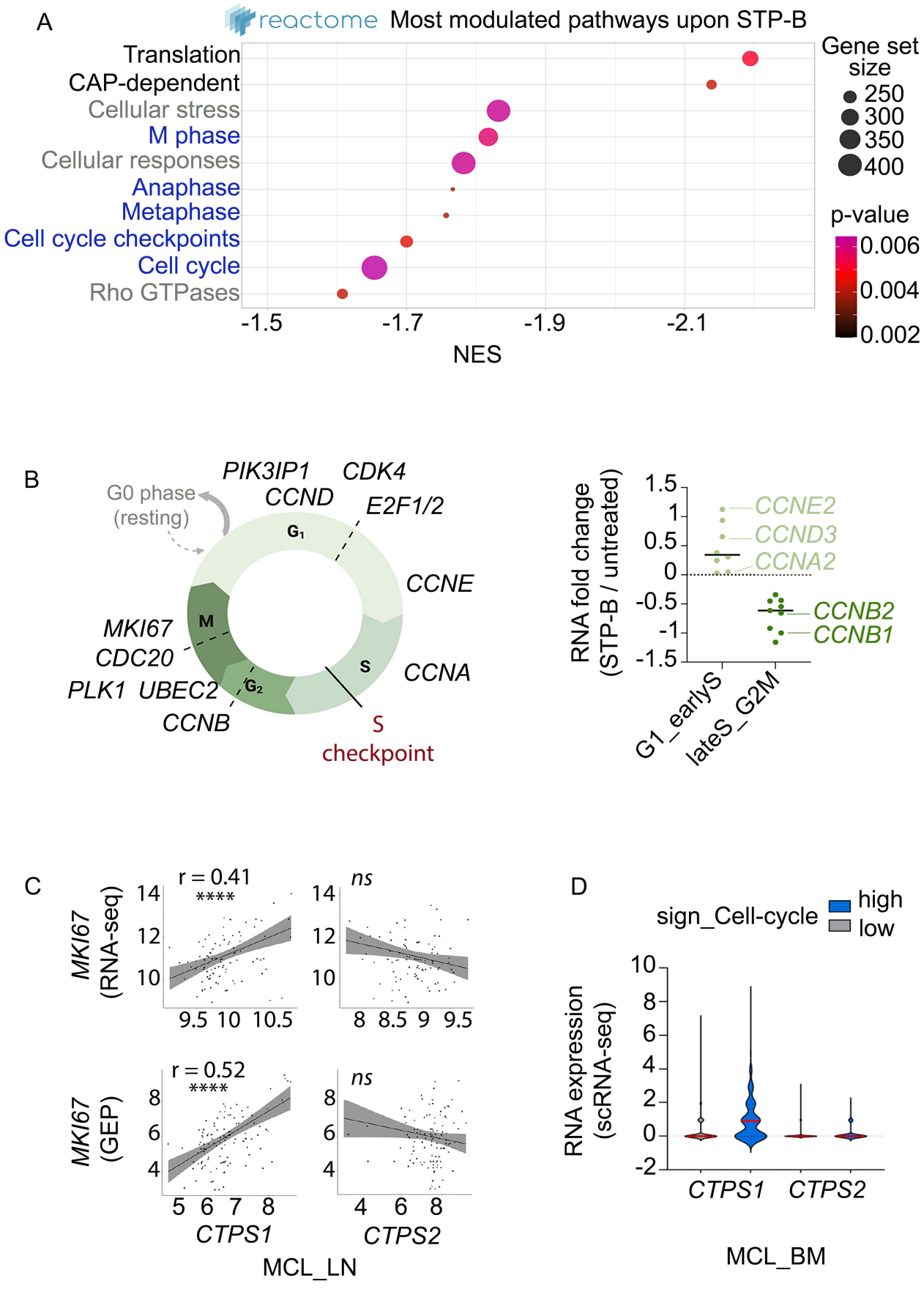
A
reactome Most modulated pathways upon STP-B
Translation
CAP-dependent
Cellular stress
M phase
Cellular responses
Anaphase
Metaphase
Cell cycle checkpoints
Cell cycle
Rho GTPases
-1.5
-1.7
-1.9
-2.1
NES
Gene set size
250
300
350
400
p-value
0.006
0.004
0.002
B
G0 phase (resting)
PIK3IP1
CDK4
CCND
E2F1/2
G1
CCNE
MKI67
CDC20
PLK1
UBEC2
CCNB
M
G2
S
CCNA
S checkpoint
RNA fold change (STP-B / untreated)
1.5
1
0.5
0
-0.5
-1
-1.5
CCNE2
CCND3
CCNA2
CCNB2
CCNB1
G1_earlyS
lateS_G2M
C
MKI67 (RNA-seq)
r = 0.41
****
ns
MKI67 (GEP)
r = 0.52
****
ns
CTPS1
CTPS2
MCL_LN
D
sign_Cell-cycle
high
low
RNA expression (scRNA-seq)
CTPS1
CTPS2
MCL_BM

Figure 4

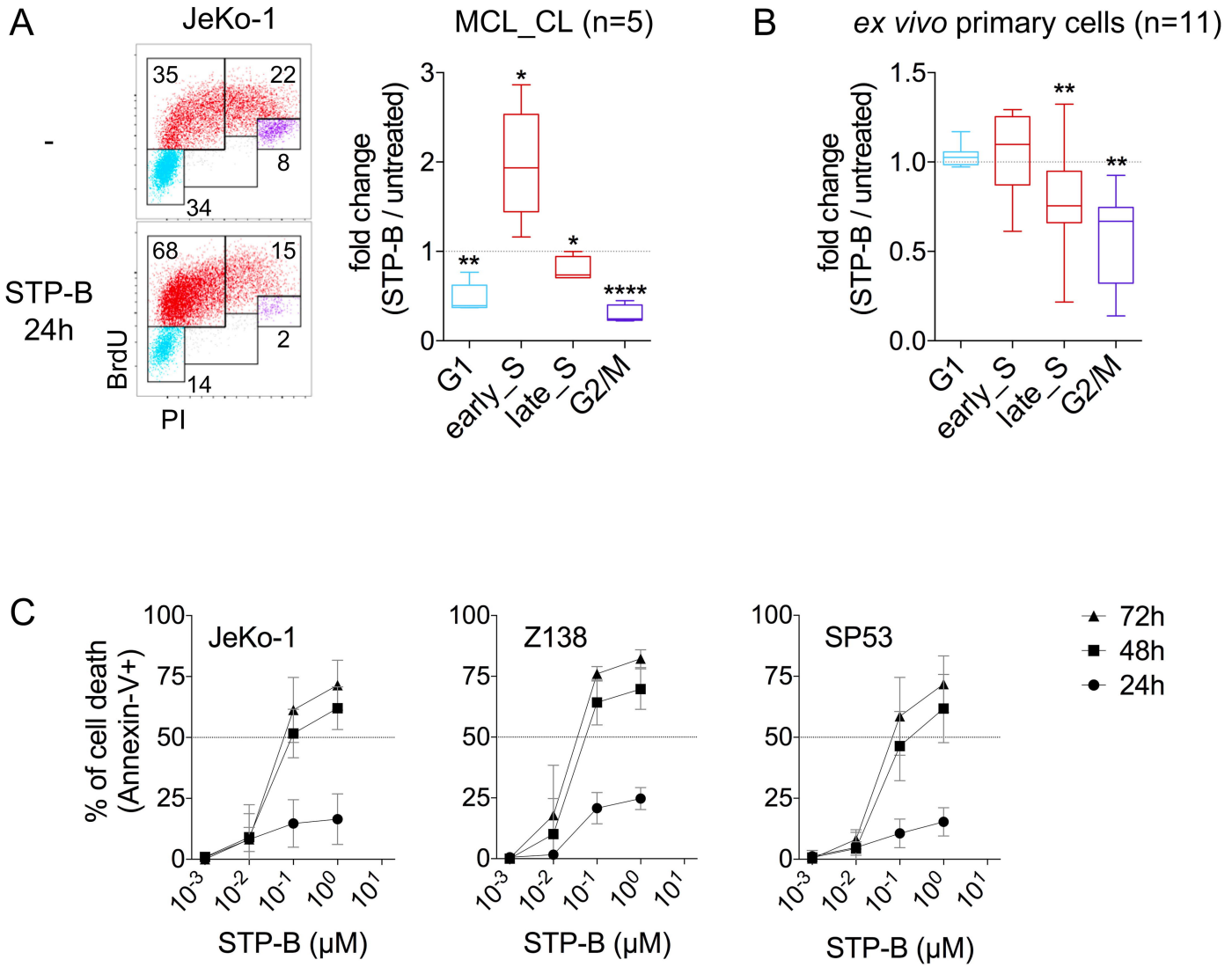
A
JeKo-1
-
STP-B
24h
BrdU
PI
35
22
8
34
68
15
2
14
MCL_CL (n=5)
fold change
(STP-B / untreated)
G1
early_S
late_S
G2/M
B
ex vivo primary cells (n=11)
C
JeKo-1
Z138
SP53
% of cell death
(Annexin-V+)
STP-B (μM)
72h
48h
24h

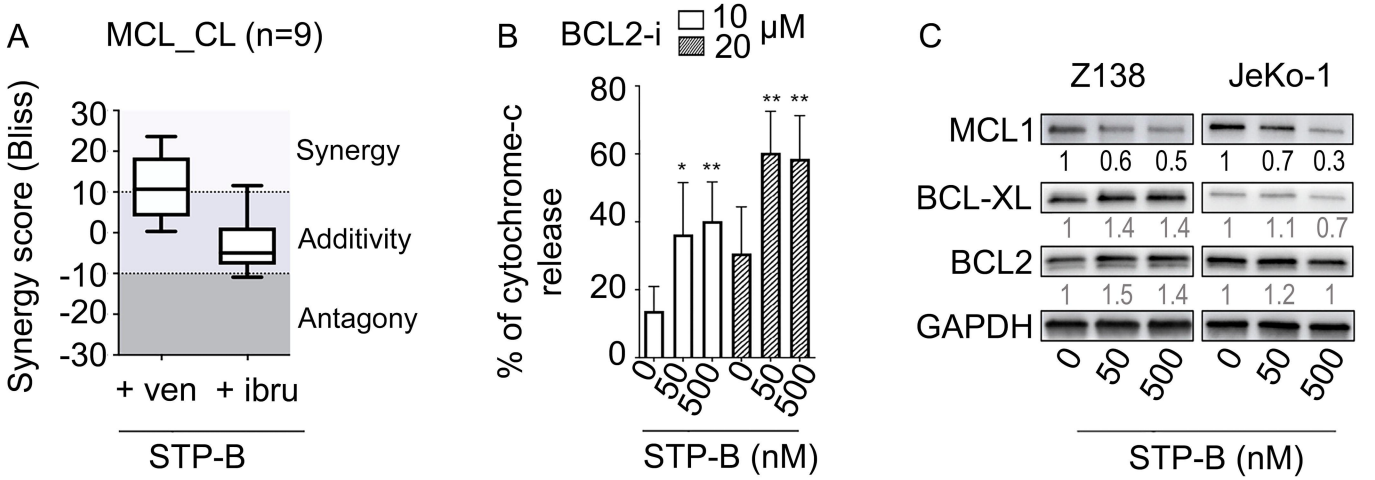
A
MCL_CL (n=9)
Synergy score (Bliss)
30
20
10
0
-10
-20
-30
Synergy
Additivity
Antagony
+ ven
+ ibru
STP-B
B
BCL2-i
10
20
μM
% of cytochrome-c release
80
60
40
20
0
* * ** **
0 50 500 0 50 500
STP-B (nM)
C
Z138
JeKo-1
MCL1
1 0.6 0.5 1 0.7 0.3
BCL-XL
1 1.4 1.4 1 1.1 0.7
BCL2
1 1.5 1.4 1 1.2 1
GAPDH
0 50 500 0 50 500
STP-B (nM)

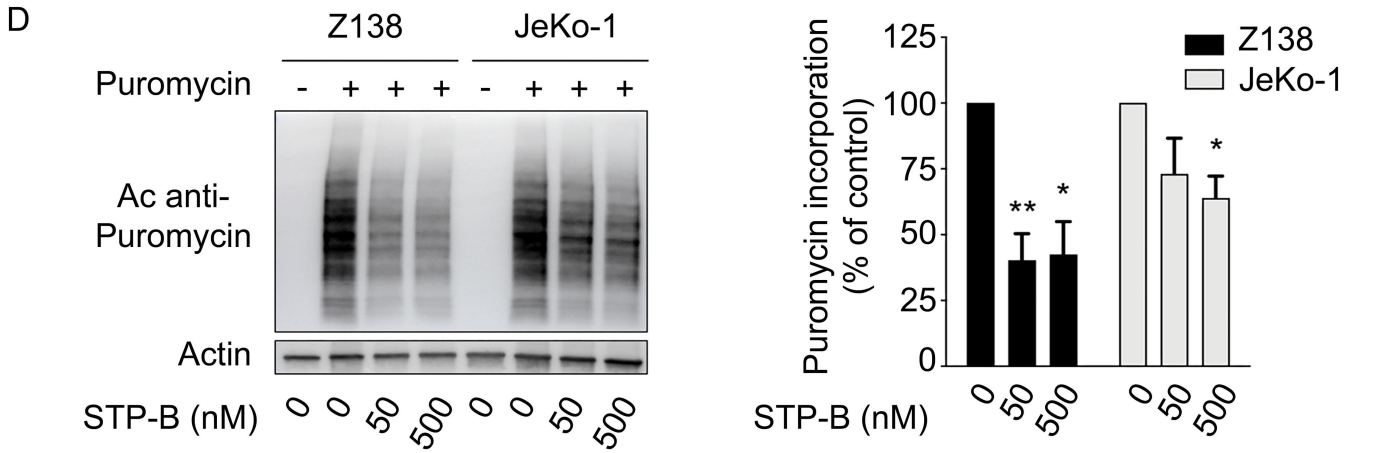
D
Z138
JeKo-1
Puromycin
- + + + - + + +
Ac anti-Puromycin
Actin
STP-B (nM)
0 0 50 500 0 0 50 500
Puromycin incorporation (% of control)
125
100
75
50
25
0
Z138
JeKo-1
** *
* *
0 50 500 0 50 500
STP-B (nM)

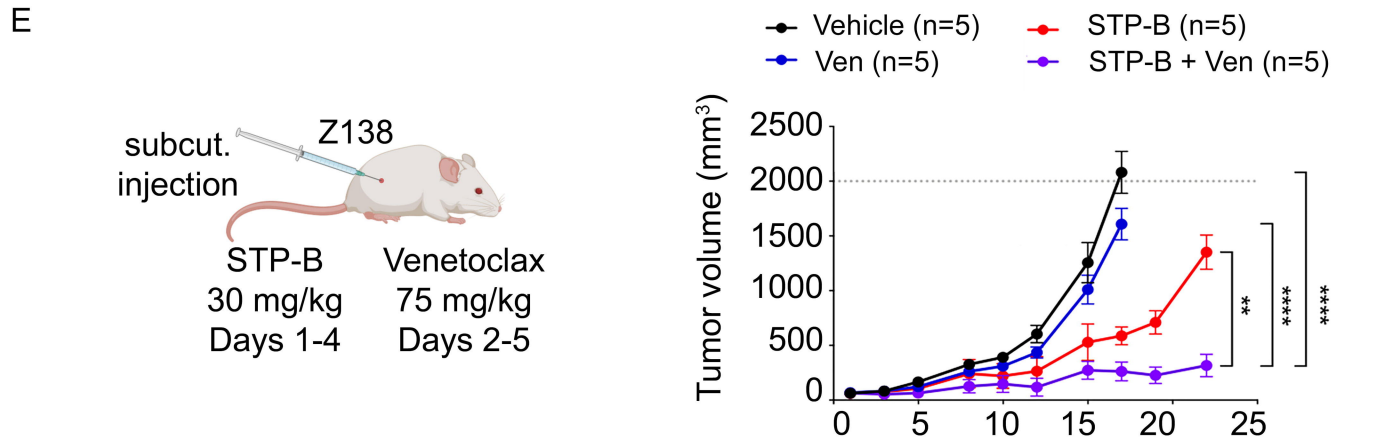
E
subcut. injection
Z138
STP-B
30 mg/kg
Days 1-4
Venetoclax
75 mg/kg
Days 2-5
Vehicle (n=5)
Ven (n=5)
STP-B (n=5)
STP-B + Ven (n=5)
Tumor volume (mm3)
2500
2000
1500
1000
500
0
0 5 10 15 20 25
**
****
****

Figure 5

Selective pharmacologic targeting of CTPS1 shows single-agent activity and synergizes with BCL2 inhibition in aggressive mantle cell lymphoma

This supplementary file contains supplementary Methods, supplementary references, supplementary Table S1, supplementary Figures S1-6 and associated legends.

Supplemental Methods

Cell line source

MINO, REC-1, MAVER-1 and GRANTA-519 were purchased from DSMZ (Germany). Z138, JeKo-1 and JVM2 from ATCC (USA). UPN1, HBL2 and SP53 were kindly provided by Prof. V. Ribrag (Institut Gustave Roussy, France), Prof. M. Callanan (University of Burgundy, France) and Prof. S. Chen-Kiang (Cornell University, NY), respectively. NTS3 cell line has been generated in our laboratory (characterized by GEP, GSE86322). Resistant cell lines were generated using *in vitro* selection and named -VenR and -IbruR for venetoclax and ibrutinib resistance, respectively. HLA-A, -B, and -C typing was carried out by Next-Generation-Sequencing (NGS) using Omixon Holotype HLA® (Omixon, Budapest, Hungary, EFS Nantes).

Reagents and antibodies

STP-B, a highly selective inhibitor of CTPS1[1], was provided by Step Pharma (Saint-Genis-Pouilly, France). Venetoclax and ibrutinib were obtained from Selleck Chemicals. Anti-CD19 was purchased from Beckman Coulter, AnnexinV was from Immunotools. For immunoblotting, anti-CTPS1 and anti-CTPS2 pAbs were from Atlas Antibodies. Anti-MCL1 mAb (D35A5), anti-phospho(Ser65) 4E-BP1 mAb (174A9) and anti-4E-BP1 pAb were from Cell Signaling. Anti-BCL2 mAb (clone 7) was from BD Biosciences. Anti-BCL-XL mAb (D-3), anti-Cyclin D1 pAb (H-295) and anti-Cyclin D2 pAb (C-17) were from Santa Cruz Biotechnology. Anti-BIRC5 pAb was from R&D Systems and anti-Puromycin mAb (12D10) was from Sigma-Aldrich.

BH3 profiling assay

BH3 profiling assay was performed in MCL cell lines as previously described[2,3]. Z138 cells were pre-treated or not with 50 or 500 nM STP-B for 24 hours. Cells were permeabilized in DTEB buffer with 0.002% digitonin and exposed to 10 or 20 µM of the BCL2 specific BH3-mimetic venetoclax or DMSO (control condition) for 1 hour at 27°C, before fixation with 2% formaldehyde at room temperature for 15 min. After addition of neutralizing buffer (Tris/Glycine

buffer) for 5 min, cells were stained with anti-cytochrome c antibody (BD Biosciences) in 0.1%Saponin/1%BSA/PBS overnight at 4°C. Loss of cytochrome c was analyzed by flow cytometry by gating the cytochrome c positive population.

Puromycin incorporation assay

Puromycin incorporation (SUnSET) assay was performed using a previously established protocol[4]. Briefly, cells were pre-treated with 50 or 500 nM STP-B for 24 hours, before addition of 1 µM puromycin for 30 min. Cells were washed twice with ice-cold PBS before standard protein extraction. Puromycin incorporation was revealed by western blotting using anti-puromycin antibody diluted at 1:10000.

Animal models

Z138-xenograft subcutaneous model

Z138, an ibrutinib/venetoclax double resistant blastoid MCL cell line, was selected to evaluate the *in vivo* efficacy of STP-B alone or combined with venetoclax. Z138 cells ($5x10^6$) were injected subcutaneously into the right flank of mice. Tumor growth was measured with calipers three times a week and mice were randomized when the tumor reached approximately 50 to 150 mm^3. STP-B was dosed at 30 mg/kg/day subcutaneously days 1-4 of a 7-day cycle and venetoclax at 75 mg/kg/day orally days 2-5 of a 7-day cycle for three cycles.

MCL Patient Derived Xenograft (PDX) disseminated model

In vivo efficacy of STP-B was also evaluated using an ibrutinib-refractory $TP53^{MUT}$ MCL PDX disseminated model. PDX MCL cells ($1x10^6$) were injected intravenously into the tail vein of NSG conditioned with sublethal (1.5 Gy) total body irradiation. Treatment was initiated 1 week after transplantation: STP-B was dosed at 30 mg/kg/day subcutaneously days 1-4 of a 7-day cycle for three cycles. At weeks 2 and 3 post-injection, blood sample from each mouse was taken by tail vein puncture in heparin tube and percentage of MCL cells in the peripheral blood was measured by flow cytometry using human CD45 staining.

Supplemental References

1. Asnagli H, Minet N, Pfeiffer C, et al. CTP Synthase 1 Is a Novel Therapeutic Target in Lymphoma. *HemaSphere*. 2023;7(4):.
2. Chiron D, Bellanger C, Papin A, et al. Rational targeted therapies to overcome microenvironment-dependent expansion of mantle cell lymphoma. *Blood*. 2016;128(24):2808–2818.
3. Decombis S, Bellanger C, Le Bris Y, et al. CARD11 gain of function upregulates BCL2A1 and promotes resistance to targeted therapies combination in B-cell lymphoma. *Blood Journal*. 2023;blood.2023020211.
4. Ravi V, Jain A, Mishra S, Sundaresan NR. Measuring Protein Synthesis in Cultured Cells and Mouse Tissues Using the Non-radioactive SUnSET Assay. *CP Molecular Biology*. 2020;133(1):e127.

STP	**IC50 values (µM)**		RNA-Seq (log2)*		TP53	Other Drug responses	
MCL cell lines	Mean	SEM	*CTPS1*	*CTPS2*	STATUS	Venetoclax	Ibrutinib
Z138_WT	0.015	0.005	*ND*	*ND*	WT	R	R
Z138 p53 KO1	0.014	0.003	*ND*	*ND*	**KO**	R	R
Z138 p53 KO2	0.011	0.002	*ND*	*ND*	**KO**	R	R
JEKO	0.036	0.001	1,0	1,0	Mutated	R	S
JEKO-IbruR	0.028	0.002	1,0	1,0	Mutated	R	**R**
MAVER	0.22	0.07	1,0	1,0	Mutated	S	R
MAVER-VenR	0.29	0.12	1,0	0,9	Mutated	**R**	R
MINO	> 3.0	-	1,0	1,0	Mutated	S	S
MINO-VenR	> 3.0	-	1,0	1,0	Mutated	**R**	S
MINO-IbruR	> 3.0	-	0,9	1,0	Mutated	S	**R**

Table S1: Isogenic resistant cell lines characteristics.
CTPS1/2 levels are relative to the parental cell line. R: resistant (IC_{50} > 1000nM), S: sensitive (IC_{50} < 1000nM), ND: not determined

Supplemental Figure Legends

Figure S1: B-cell lymphoma cells relies on CTPS1 to proliferate.

A: Immunoblotting of CTPS1 and CTPS2 was performed in 6 MCL cell lines. Both anti-CTPS1 and anti-CTPS2 antibodies (Atlas Antibodies) were used at a dilution of 1:1000. Secondary antibody (goat anti-rabbit) was used at a dilution of 1:5000. Exposure times were 4 and 20 seconds for CTPS1 and CTPS2 respectively. Protein levels relative to GAPDH level are indicated.

B: Dependence to *CTPS1* and *CTPS2* was evaluated in 70 B-cell lymphoma cell lines using the DepMap CRISPR dataset.

Figure S2: Sensitivity to STP-B is independent of *CTPS1/2* expression, resistance to BTK/BCL2 targeted therapies and *TP53* status.

A: *CTPS1/2* expression from 3'SRP data was compared with STP-B IC_{50} values in 10 MCL cell lines. Spearman test was used.

B: STP-B IC_{50} values were compared in MCL cell lines depending on *TP53* status, sensitivity (S) or resistance (R) to venetoclax and ibrutinib (see Table 1 for more details). Mann-Whitney test was used.

C: Resistance of Jeko-IbruR and Maver-VenR sublines was validated by CTG assay and Z138 $TP53^{KO}$ clones confirmed their resistance to Nutlin3a-induced cell death.

Figure S3: STP-B is well tolerated in mouse models

A: The body weight variation of (n=5) control and (n=5) treated mice was evaluated upon STP-B (30 mg/kg) treatment.

B: Mouse PBMC count was determined by flow cytometry (huCD45-negative count) 21 days and 28 days after engraftment. Mann-Whitney test was used.

Figure S4: Transcriptomic analysis of MCL cells was performed in response to STP-B.

A: The heat-map highlights the transcriptional clustering of 9 MCL cell lines treated (STP-B) or not (CT) with STP-B IC_{50} for 24 hours.

B: The volcano-plot represents the differentially expressed (DE) genes upon STP-B treatment in 9 MCL cell lines. Dotted lines indicate the cut-off for significance (Log_2 FC < -0.5 or > 0.5 and adjusted p-value < 0.05). The greatest regulated genes (red dots) are annotated on the graph.

Figure S5: CTPS1 inhibition synergizes with venetoclax

A: STP-B and ibrutinib combination efficacy was evaluated in 9 MCL cell lines. Cells were treated for 72 hours with 3 concentrations of STP-B and ibrutinib as indicated. Combination inhibitory effect was assessed by CTG assay. Red: most synergistic area, green: lowest synergistic area. Bliss synergy score is indicated.

B: STP-B and venetoclax combination efficacy was evaluated in 9 MCL cell lines. Cells were treated for 72 hours with 3 concentrations of STP-B and venetoclax as indicated in each graph. Cell death was determined by Annexin-V staining.

Figure S6: CTPS1 inhibition led to translation inhibition and consequent decrease of MCL1 protein level.

A: MCL1 mRNA and protein levels were determined by quantitative PCR and immunoblotting following treatment with 50 or 500 nM STP-B for 24 hours in Z138 and JeKo-1. Each graph represents 3 independent experiments.

B: CCND1, CCND2 and BIRC5 protein expression was determined by immunoblotting upon STP-B treatment.

C: CCND1, CCND2 and BIRC5 protein levels were normalized to GAPDH levels and gene expression was assessed by 3'SRP upon STP-B treatment.

D: Phospho(Ser65)-4E-BP1 and 4E-BP1 protein levels were assessed in Z138 and JeKo-1 cells treated for 24 hours with STP-B. Protein levels relative to tubulin level are indicated.

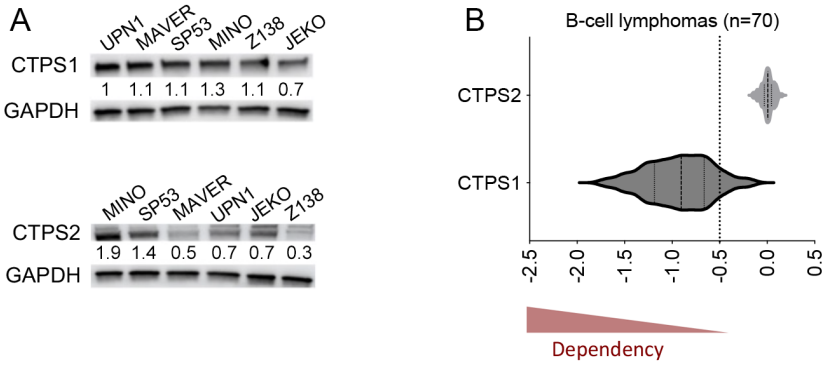
A
UPN1
MAVER
SP53
MINO
Z138
JEKO
CTPS1
1 1.1 1.1 1.3 1.1 0.7
GAPDH
MINO
SP53
MAVER
UPN1
JEKO
Z138
CTPS2
1.9 1.4 0.5 0.7 0.7 0.3
GAPDH
B
B-cell lymphomas (n=70)
CTPS2
CTPS1
-2.5
-2.0
-1.5
-1.0
-0.5
0.0
0.5
Dependency

Figure S1

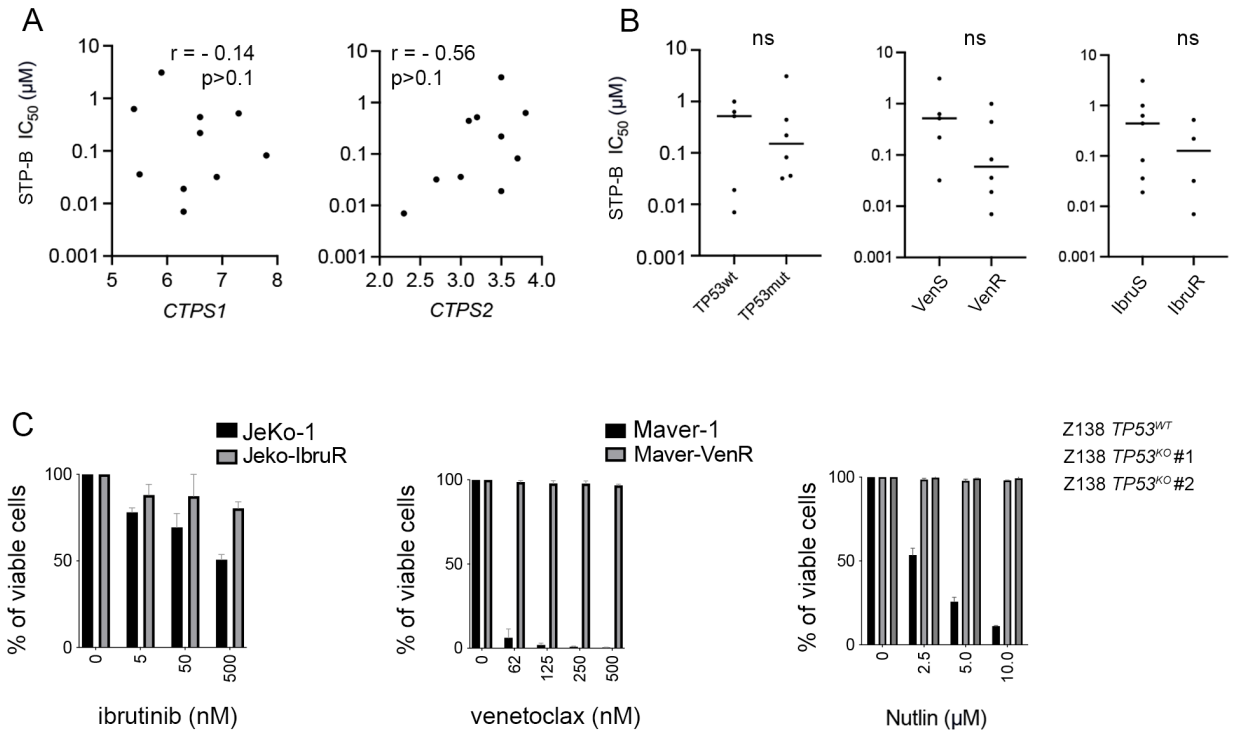
A
STP-B IC50 (μM)
r = - 0.14
p>0.1
CTPS1
r = - 0.56
p>0.1
CTPS2
B
ns
TP53wt
TP53mut
VenS
VenR
IbruS
IbruR
C
JeKo-1
Jeko-IbruR
% of viable cells
ibrutinib (nM)
Maver-1
Maver-VenR
venetoclax (nM)
Z138 TP53WT
Z138 TP53KO#1
Z138 TP53KO#2
Nutlin (μM)

Figure S2

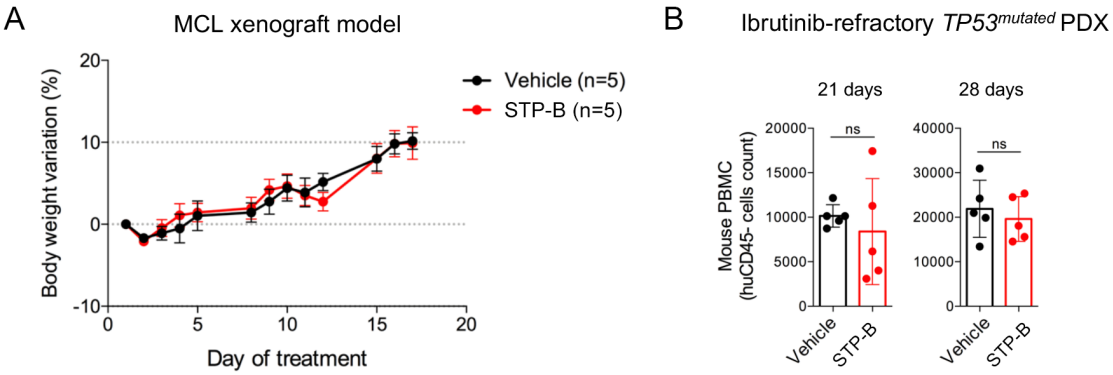
A
MCL xenograft model
Body weight variation (%)
Day of treatment
Vehicle (n=5)
STP-B (n=5)
B
Ibrutinib-refractory TP53mutated PDX
21 days
28 days
Mouse PBMC (huCD45- cells count)
ns
ns
Vehicle
STP-B
Vehicle
STP-B

Figure S3

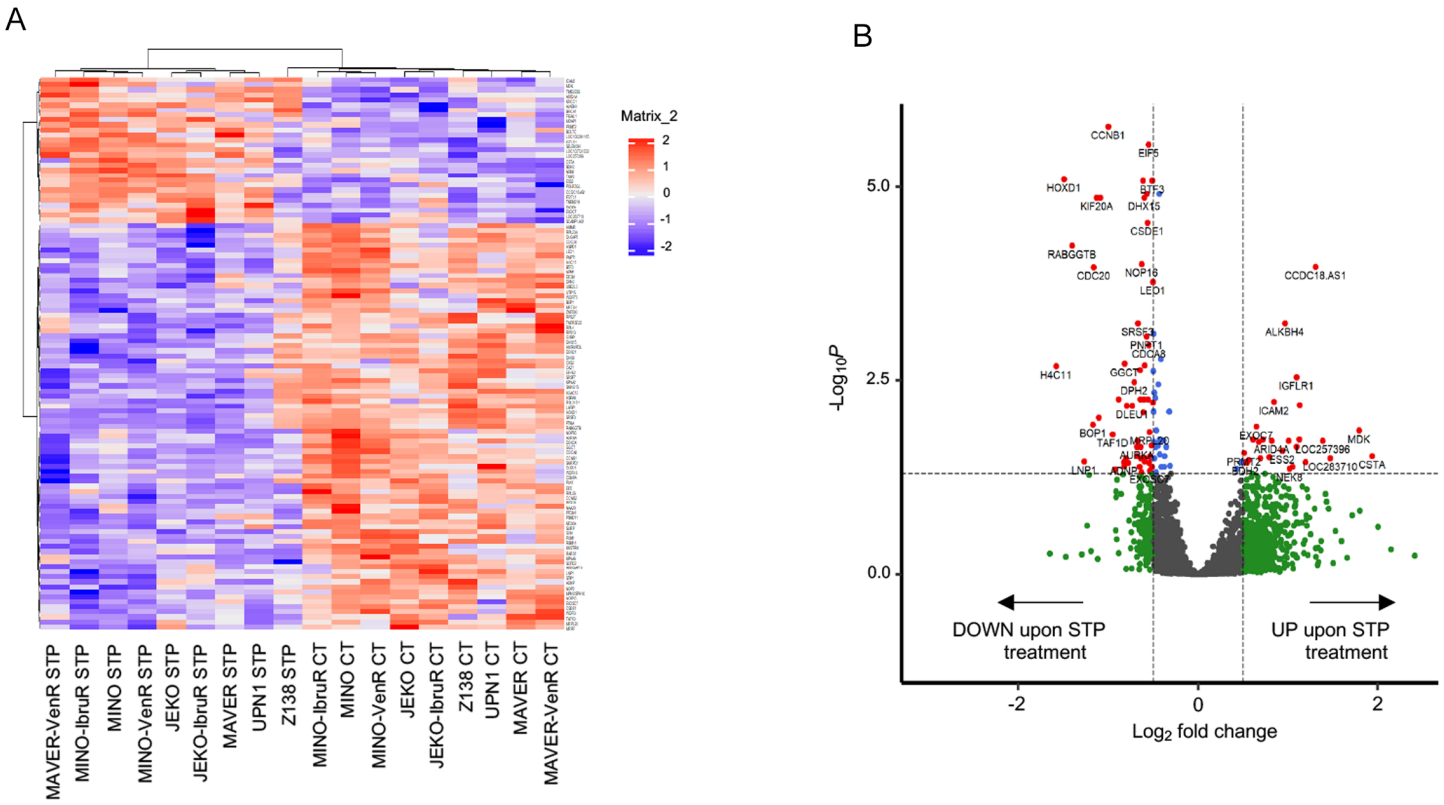
A
Matrix_2
2
1
0
-1
-2
MAVER-VenR STP
MINO-IbruR STP
MINO STP
MINO-VenR STP
JEKO STP
JEKO-IbruR STP
MAVER STP
UPN1 STP
Z138 STP
MINO-IbruR CT
MINO CT
MINO-VenR CT
JEKO CT
JEKO-IbruR CT
Z138 CT
UPN1 CT
MAVER CT
MAVER-VenR CT
B
-Log10P
5.0
2.5
0.0
CCNB1
EIF5
HOXD1
BTF3
KIP20A
DHX15
CSDE1
RABGGTB
CDC20
NOP16
LED1
CCDC18.AS1
ALKBH4
SRSF3
PNRT1
CDCA8
H4C11
GGCT
IGFLR1
DPH2
ICAM2
DLEU1
BOP1
TAF1D
MRPL20
EXOC7
MDK
AURKA
ARID4A
LOC257396
LNP1
ANP32E
PSMF1
ESS2
LOC283710
CSTA
BOP1
ENKD1
EXOSC5
DOWN upon STP treatment
UP upon STP treatment
-2
0
2
Log2 fold change

Figure S4

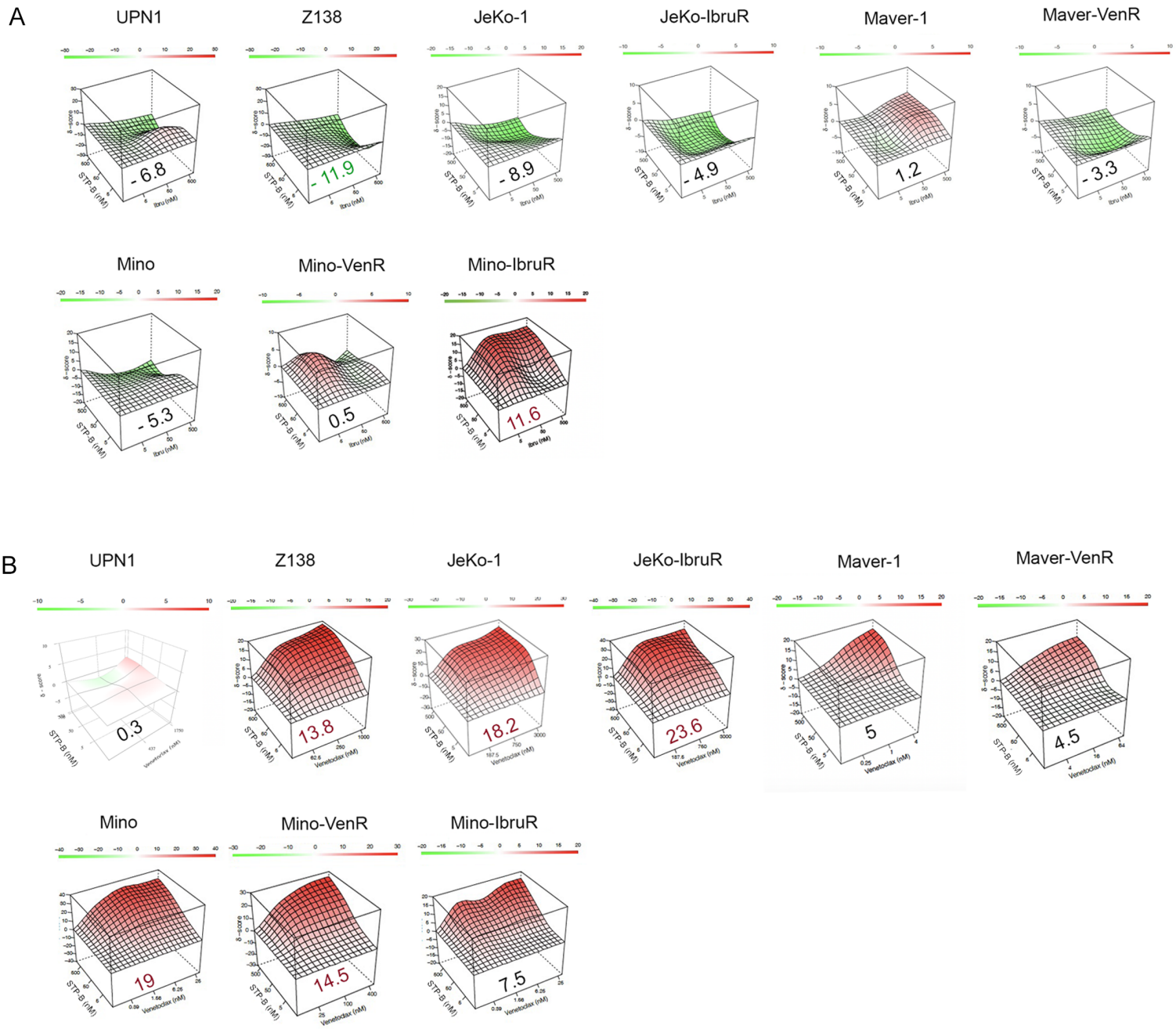
A
UPN1
Z138
JeKo-1
JeKo-IbruR
Maver-1
Maver-VenR
Mino
Mino-VenR
Mino-IbruR
- 6.8
- 11.9
- 8.9
- 4.9
1.2
- 3.3
- 5.3
0.5
11.6
B
UPN1
Z138
JeKo-1
JeKo-IbruR
Maver-1
Maver-VenR
Mino
Mino-VenR
Mino-IbruR
0.3
13.8
18.2
23.6
5
4.5
19
14.5
7.5

Figure S5

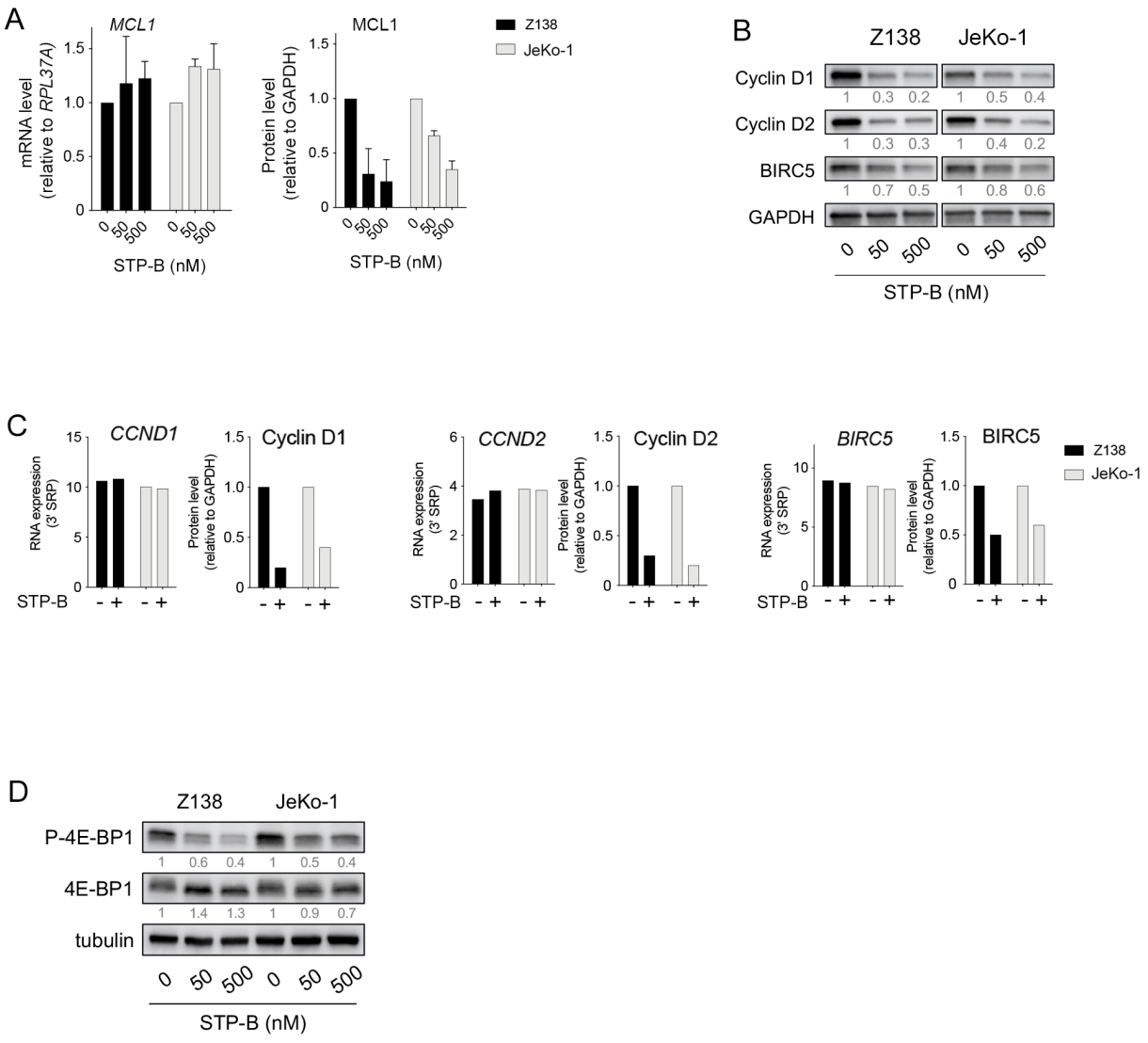
A
MCL1
mRNA level (relative to RPL37A)
STP-B (nM)
MCL1
Protein level (relative to GAPDH)
STP-B (nM)
Z138
JeKo-1
B
Z138
JeKo-1
Cyclin D1
Cyclin D2
BIRC5
GAPDH
STP-B (nM)
C
CCND1
RNA expression (3' SRP)
Cyclin D1
Protein level (relative to GAPDH)
CCND2
Cyclin D2
BIRC5
BIRC5
STP-B
Z138
JeKo-1
D
Z138
JeKo-1
P-4E-BP1
4E-BP1
tubulin
STP-B (nM)

Figure S6